
Article:
Ritterskamp, D., Bearup, D. orcid.org/0000-0001-8524-7659 and Blasius, B. (2016) Emergence of evolutionary cycles in size-structured food webs. Journal of Theoretical Biology. ISSN 0022-5193

https://doi.org/10.1016/j.jtbi.2016.08.024

www.elsevier.com/locate/yjtbi

Emergence of evolutionary cycles in size-structured food webs

Daniel Ritterskamp, Daniel Bearup, Bernd Blasius

PII: S0022-5193(16)30258-2
DOI: http://dx.doi.org/10.1016/j.jtbi.2016.08.024
Reference: YJTBI8792

To appear in: *Journal of Theoretical Biology*

Received date: 15 February 2016
Revised date: 18 July 2016
Accepted date: 12 August 2016

Cite this article as: Daniel Ritterskamp, Daniel Bearup and Bernd Blasius Emergence of evolutionary cycles in size-structured food webs, *Journal o Theoretical Biology,* http://dx.doi.org/10.1016/j.jtbi.2016.08.024

Emergence of evolutionary cycles in size-structured food webs

Daniel Ritterskamp[a,b,*], Daniel Bearup[b], Bernd Blasius[b]

[a] *University of Bristol, Faculty of Engineering, Merchant Venturers Building, BS8 1UB, United Kingdom*

[b] *CvO University Oldenburg, ICBM, Carl-von-Ossietzky-Strasse 9-11, 26111 Oldenburg, Germany*

Abstract

The interplay of population dynamics and evolution within ecological communities has been of long-standing interest for ecologists and can give rise to evolutionary cycles, e.g. taxon cycles. Evolutionary cycling was intensely studied in small communities with asymmetric competition; the latter drives the evolutionary processes. Here we demonstrate that evolutionary cycling arises naturally in larger communities if trophic interactions are present, since these are intrinsically asymmetric. To investigate the evolutionary dynamics of a trophic community, we use an allometric food web model. We find that evolutionary cycles emerge naturally for a large parameter ranges. The origin of the evolutionary dynamics is an intrinsic asymmetry in the feeding kernel which creates an evolutionary ratchet, driving species towards larger bodysize. We reveal different kinds of cycles: single morph cycles, and coevolutionary and mixed cycling of complete food webs. The latter refers to the case where each trophic level can have different evolutionary dynamics. We discuss the generality of our findings and conclude that ongoing evolution in food webs may be more frequent than commonly believed.

Keywords: Community Cycling, Taxon Cycles, Coevolution, Red-Queen Dynamics, Evolutionary Limit Cycles

*Corresponding author

Email addresses: daniel.ritterskamp@bristol.ac.uk (Daniel Ritterskamp), daniel.bearup@uni-oldenburg.de (Daniel Bearup), blasius@icbm.de (Bernd Blasius)

1. Introduction

One of the main goals of evolutionary ecology is to gain insights into the interplay of population dynamics and evolution, shaping the structure and dynamics of communities [13, 7]. The outcome of eco-evolutionary processes is not easy to understand from first principles, but much progress has been achieved by theoretical approaches. Of particular interest are the conditions under which eco-evolutionary processes within communities give rise to dynamic patterns. Early theoretical studies of evolutionary driven community dynamics were restricted to simple community-modules of two or three species with fixed species roles and primarily focused on temporal changes in the abundance and mean trait values of different species or populations. These works studied the influence of co-evolution on the stability of predator-prey systems [27, 3, 2], the occurrence of character displacement in models of competition mediated by a quantitative trait [38, 35, 36, 42, 41], as well as the dynamics of co-evolutionary arms races [43]. Further theoretical analysis showed that evolution can also induce temporal changes in the composition and diversity of a community and may either increase species richness, for example via speciation events [31, 11], but may also reduce species richness, for example via self-extinction through evolutionary suicide [24, 15, 25].

One major insight of these studies was that the interplay of ecological and evolutionary processes does not inevitably lead to an evolutionary equilibrium, but can lead to a situation of non-equilibrium states, characterized by sustained evolutionary change. One particularly intriguing case is that of evolutionary cycling, which is the emergence of ongoing periodic changes in species traits or community states [12, 19]. In one of the first studies of evolutionary cycling, Rummel and Roughgarden [35] suggested the appearance of community cycles, i.e. the occurrence of evolutionary cycles in the community composition going together with sustained species turnover. Rummel and Roughgarden [35] simulated the buildup of island faunas based on a model of competitive interactions mediated by bodysize as the dominant phenotypic trait. Thereby, one key ingredient for the emergence of community cycles was attributed to the asymmetry of species interactions, The resulting community cycles, sometimes referred to as taxon cycles [45, 34], describe a scenario where an island (or local habitat), which is initially occupied by a single resident, is colonised by a new invading species of larger bodysize. The invading species forces the smaller resident to evolve to smaller bodysize, while following this evolutionary movement. The resulting coevo-

lutionary arms-race towards smaller bodysizes weakens the viability of the resident which is eventually driven to extinction, leading again to a single species community. It was shown that this simple mechanism is able to describe the empirical patterns in the build-up of island faunas in the case of *Anolis* lizards in the Lesser Antilles [34] and was subsequently investigated in a series of further studies (e.g. [36, 42, 41, 24]). In these studies, it was found that community cycles are a robust model outcome, but the details of the cycles depend on the specific model assumptions. In particular, it is possible that the bodysize change of the cycle operates in the reverse direction, so that species are driven towards larger bodysizes.

Despite this progress in describing generic mechanisms of evolutionary cycling, the studies mentioned above are limited in several respects. First, most demonstrations of evolutionary community cycles are restricted to small communities, consisting of very few species. Recently, there has been much interest in the evolutionary build-up of community structure in multi-species communities [17, 6, 20, 37, 32]. However, these studies typically observed static community structures, whereas not much is known about the conditions that favour the emergence of ongoing evolutionary change and community cycling in multi-species assemblages [40, 39]. A second related question is whether larger communities can exhibit different coevolutionary processes that occur independently from each other in different community modules, possibly at different frequencies. Finally, even though community cycles have been studied extensively for competitive interactions, not much is known about their relevance in trophically structured communities. This is quite astonishing, given the striking structural similarity of allometric evolutionary food web models [7] to competition models on a niche axis [35, 41].

One of the first allometric evolutionary food web models was introduced by Loeuille and Loreau [20] and several variants were studied in great detail [21, 20, 4, 8, 5]. In this model class, similar to (Rummel and Roughgarden [35, 36]), each species is characterized by its bodysize as a major phenotypic trait, the interactions between species are determined by their differences in bodysize, and allometric relations are considered explicitly. The essential new ingredient of allometric food web models is that they not only consider competition between species of similar bodysize, but also incorporate trophic interactions between species, so that a large species is able to prey upon smaller species. Given the strong similarity between these two model classes and the fact that predator-prey interactions are naturally asymmetric, one would expect that evolutionary community cycles, similar to taxon

cycles in models of competition, are a typical outcome in evolutionary food web models. However, while several other studies have reported evolutionary dynamics in such models, e.g. irregular extinction cascades [5], trophic outbursts [30] and Red Queen dynamics in two species communities [46], to date there has been no rigorous investigation of evolutionary cycling in this framework.

In this study, we revisit the well-studied evolutionary allometric food web model by Loeuille and Loreau [20]. We show that this model can indeed produce evolutionary cycles in a large parameter range and that the possibility of evolutionary cycles is related to the competition between species. When Loeuille and Loreau [20] introduced this model, they found food webs that are relatively invariant over time. While these results proved to be robust to a broad range of feeding ranges and competition strength, the rest of the parameter space was relatively unexplored. In particular, the parameter governing the bodysize distance over which morphs can compete, the competition range, was limited to rather small values. While some biological justification for this range was given, we argue here that this range may be too small. If competition between species arises from niche overlap (sensu MacArthur and Levins [22]), we should expect a competition range that is significantly broader and is of the same order as the feeding range of a species. This would allow inter-species competition to have a much stronger effect on the evolutionary dynamics.

Motivated by this observation, we numerically investigate the evolutionary behaviour in the model [20], by systematically varying the strength and range of the competition between species. Our simulations show that evolutionary cycling, where species are driven towards larger bodysizes, is naturally present in the model considered – not only between single species but also in large trophic communities. Thereby, we observe a plethora of regimes with distinct dynamics. Besides static food webs, we observe evolutionary single morph cycles, complex community cycles where different trophic levels undergo separate coevolutionary cycles, as well as transient dynamics. Using invasion analysis and Pairwise Invasibility Plots (PIPs) we are able to support the numerical observations, which allows us to explain the mechanism underlying the evolutionary cycles. Our findings imply that ongoing evolution in food webs may be more frequent than commonly believed.

2. Model

We follow the evolutionary food web model by Loeuille and Loreau [20]. The model considers one basal resource, such as an inorganic nutrient, ($i = 0$) and a variable number of evolving morphs ($i = 1, ..., N$). We use the term morph, rather than species, since we are not considering the speciation process. Each morph is described by its population biomass density B_i and bodysize z_i. The resource has a total density B_0 and is associated with a non-evolving 'bodysize', which is fixed to the value $z_0 = 0$. The model consists of two components: population dynamics and evolutionary dynamics, each of which operate on different time scales. The population dynamics describe the trophic interactions among morphs and determine their respective growth, survival or extinction. On a longer time-scale, usually after the population dynamics have reached an attractor, new morphs are added to the community by an evolutionary algorithm.

2.1. Population dynamics

The change of biomass B_i of morph i is given by the Lotka-Volterra equations, accounting for reproduction, intrinsic mortality, and losses due to predation and interference competition [20]

$$\frac{dB_i}{dt} = B_i\Big(\underbrace{f(z_i)\sum_{j=0}^{N}\gamma(z_i - z_j)B_j}_{Reproduction} - \underbrace{m(z_i)}_{Mortality} - \underbrace{\sum_{j=0}^{N}\gamma(z_j - z_i)B_j}_{Predation\ loss} - \underbrace{\sum_{j=1}^{N}\alpha(|z_i - z_j|)B_j}_{Competition}\Big). \tag{1}$$

Here, the intrinsic mortality $m(z_i) = m_0\ z_i^{-0.25}$ and the production efficiency $f(z_i) = f_0\ z_i^{-0.25}$ scale according to allometric relations with bodysize [26]. The function $\gamma(z_i - z_j)$ describes the consumption rate exerted by predator i on prey j. The model assumes that the feeding efficiency decays with the bodysize difference as a one tailed Gaussian function

$$\gamma(z_i - z_j) = \begin{cases} \frac{\gamma_0}{\sigma\sqrt{2\pi}}\exp\Big(-\frac{(z_i - z_j - d)^2}{\sigma^2}\Big), & z_i > z_j, \\ 0, & z_i \leq z_j, \end{cases} \tag{2}$$

where d is the optimal predator-prey bodysize distance, γ_0 can be used to scale the maximal consumption strength, and σ describes the feeding range

of a morph (i.e., the Gaussian function has standard deviation of $\sigma/\sqrt{2}$). The cut-off for $z_i \leq z_j$ in the feeding kernel implies that a predator is only able to consume prey with a strictly smaller bodysize. This causes an asymmetry in trophic interactions, giving the larger of two similar sized morphs a small advantage since it can consume, but cannot be consumed by, the smaller one. Additionally, we also tested a smooth feeding kernel. Our numerical simulations revealed that our main conclusions are valid also for a smooth, but asymmetrical feeding kernel (see Fig A.7).

The function $\alpha(|z_i - z_j|)$ describes interference competition between two morphs i and j. It is modelled as a symmetric rectangular function (the competition kernel) of bodysize differences

$$\alpha(|z_i - z_j|) = \begin{cases} \alpha_0, & |z_i - z_j| < \beta, \\ 0, & |z_i - z_j| \geq \beta, \end{cases} \tag{3}$$

where α_0 is the competition strength and β the competition range.

The change in the density of the resource $i = 0$ follows a chemostat equation

$$\begin{aligned} \frac{dB_0}{dt} =& I - eB_0 - \sum_{j=1}^{N} \gamma(z_j) B_j \, B_0 + \nu \sum_{j=1}^{N} \sum_{i=1}^{N} \alpha(|z_j - z_i|) B_j B_i \\ &+ \nu \sum_{j=1}^{N} m(z_j) B_j + \nu \sum_{j=1}^{N} \sum_{i=1}^{N} (1 - f(z_j)) \gamma(z_j - z_i) B_j B_i, \end{aligned} \tag{4}$$

consisting of a constant resource inflow I, a relative outflow of rate e, losses due to consumption by morphs, and three terms describing the recycling of a fraction ν of dead biomass from interference competition, intrinsic mortality, and consumption.

In this model, the interaction kernels for feeding and competition are both discontinuous. This discontinuity could influence the population dynamics and thus the evolutionary behaviour. However, we find that our results are qualitatively unchanged when these discontinuous functions are replaced with continuous functions (see Fig A.7).

2.2. Evolutionary dynamics

The system is initialized with the resource (trait value $z_0 = 0$ and initial biomass $B_0 = I/e$) and a single evolving morph of bodysize $z_1 = d$,

corresponding to a maximal consumption rate on the resource. Each morph mutates at a constant rate of ω_0 per unit biomass and unit time. At each mutation event of a morph k, a new morph is added to the system with bodysize z_M that is randomly chosen from the mutation interval $[0.8\, z_k, 1.2\, z_k]$. This interval is centred around, and increases linearly with, the bodysize of the mutating morph z_k. The new morph is introduced with an initial biomass of θ, which is also the extinction threshold. If due to the population dynamics the biomass B_k of any morph falls below this threshold θ, it is considered extinct and removed from the system.

2.3. Parameter values, implementation, and cycle detection

We varied the range β and the strength α_0 of the competition kernel as our main control parameters. The other model parameters are fixed to: $f_0 = 0.3$, $m_0 = 0.1$, $\gamma_0 = 1/\sqrt{2}$, $d = 2$, $I = 10$, $e = 0.1$, $\nu = 0.5$, and $\sigma = \sqrt{2}$. In contrast to Loeuille and Loreau [20] we increased the extinction threshold from $\Theta = 10^{-20}$ to $\Theta = 10^{-10}$ (see also Allhoff and Drossel [4]) and the mutation rate from $\omega_0 = 10^{-6}$ to $\omega_0 = 10^{-5}$. Our robustness tests showed that these deviations from the original model formulation have no effect on the model outcome, but they allowed us to substantially increase the evolutionary time considered over our simulation runs. If not stated elsewhere, the simulations were carried out over 10^9 time-units. Numerical simulations were performed using a Runge-Kutta-Fehlberg method 4/5 [28] which was implemented in C++.

We say that we observe an evolutionary cycle if a simulated time series contains at least one whole period of a cycle after an initial build up phase of 10^8 time-units. Therefore, the maximal observable period length is limited by the remaining $9 \cdot 10^8$ time-units. If the period length of a cycle is close to this limit, cycling is difficult to detect and can depend on the build-up phase. To aid detection, we consider 5 realisations per parameter set with different seeds for the random numbers in the evolutionary algorithm. If any of these runs displays cycling we classify the parameter set as producing cycling behaviour. Thus, the distinction between static and cycling food webs depends on the time interval and the threshold condition (one period) used, especially in the transition regions.

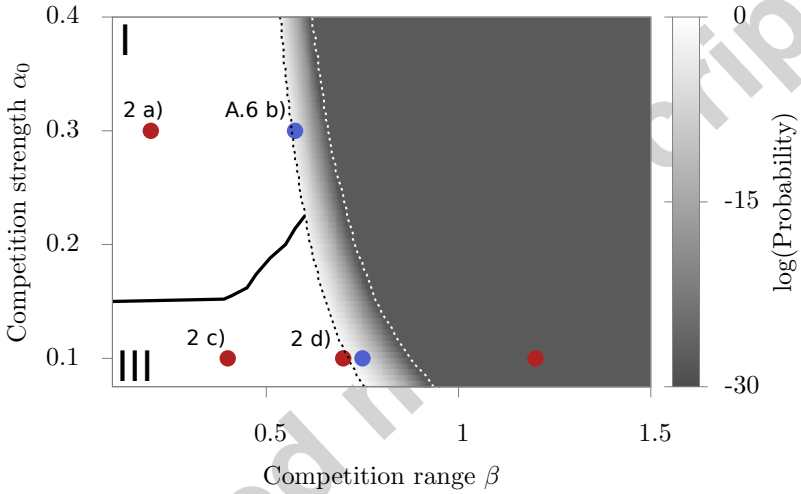

Figure 1: Map of the evolutionary behaviour in dependence of the competition parameters. The map splits into four regions of distinct dynamic behaviour: Static food webs (region I), single morph cycles (region II), complex community dynamics (region III), and a transition regime in which single morph cycles occur but the system eventually becomes polymorphic (region IV). The black solid line separates the regions of static (region I) and cyclic (region III) polymorphic food webs and is obtained from numerical simulations. The grey scale indicates the probability P for a monomorphic system to become dimorphic during one cycle period and is calculated by analysis of the invasion fitness in a monomorphic system (see section 3.2). The black dotted line shows the isocline of $P = 1$. To the right of this line single morph cycles can occur. The white dotted line indicates the isocline of $\log P = -30$ and separates regions II and IV. The red dots correspond to the examples shown in Fig. 2 and the blue dots to the transition states shown in Fig. Appendix A.6.

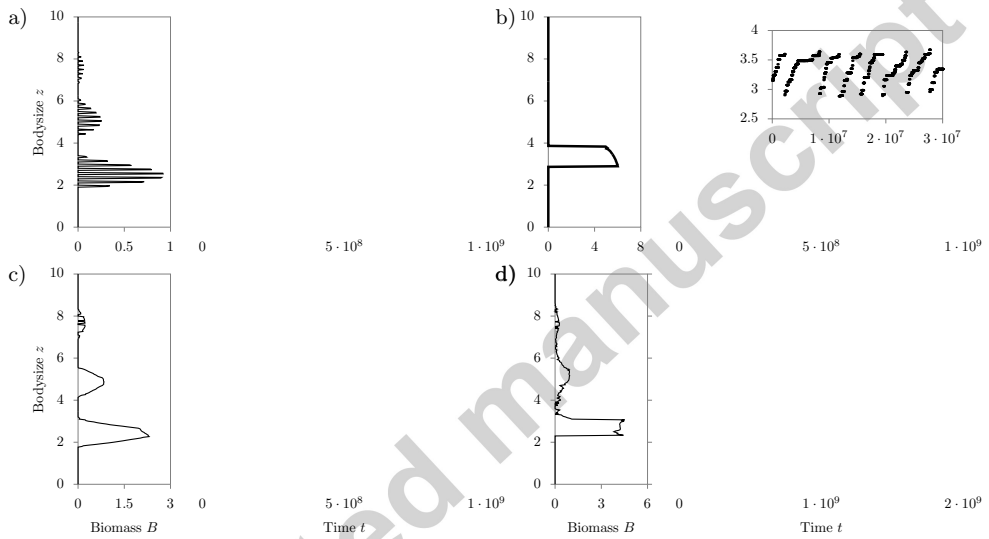

Figure 2: Evolutionary food web dynamics for different competition parameters β and α_0. Each subplot (**a-d**) corresponds to the parameter combination of a red point in Fig. 1 and shows the time evolution of bodysizes of all morphs after the initial build-up phase (right) and the corresponding biomass-bodysize histograms (left). **a**) Static food web, as in [20], for $\alpha_0 = 0.3$ and $\beta = 0.2$. **b**) Single morph cycles ($\alpha_0 = 0.1$ and $\beta = 1.2$). The inset shows a close-up of the simulated cycle in bodysize for a shorter time range. **c**) Complex community dynamics, showing different coevolutionary cycles in each trophic level ($\alpha_0 = 0.1$ and $\beta = 0.4$). The vertical lines mark time-points at which the two largest morphs in the lowest trophic level are within competition range. **d)** Mixed evolutionary cycle, showing the coexistence of a single morph cycle in the lowest trophic level and coevolutionary cycles in the higher trophic levels ($\alpha_0 = 0.1$ and $\beta = 0.7$).

3. Results

3.1. Numerical simulations, revealing four dynamics regions

We used numerical simulations to study the dependence of the evolutionary dynamics of the food web model on inter-species competition. Exploring the parameter space (β, α_0) of the competition kernel, we identified four distinct behavioural regimes (regions I - IV). The regions in which each of these behaviours occur are presented in Fig. 1 and exemplary time series for all regimes are shown in Figs. 2 and A.6. Region I is characterized by the build-up of evolutionary and convergence stable food webs, as introduced by Loeuille and Loreau [20]. Region II exhibits single morph cycles. In this region the community is composed of the resource and a monomorphic consumer with a bodysize that is not constant but undergoes evolutionary cycles within a narrow range. Region III features complex community dynamics. This region is characterized by co-occurring single morph and polymorphic coevolutionary cycles that cover several trophic layers. Region IV is a transition area in which an initial period of single morph cycles eventually gives way to a polymorphic community. The resulting food webs can be evolutionarily static or dynamic. Our numerical simulations showed that the map of evolutionary outcomes in Fig. 1 is generic towards parameter variation (e.g. σ, γ_0). That is, while the size of the regions may change, as long as the parameters chosen allow trophic structure each of these types of behaviour can be found. We consider each state, and the transition between states, in more detail below.

Static food webs: region I. For small competition ranges β and high competition strengths α_0 (region I) we obtain food webs that are close to an evolutionarily and convergence stable state. This is exactly the behaviour observed by Loeuille and Loreau [20]. Fig. 2a shows an example time series for a static food web and its distribution of biomass relative to bodysize. After an initial build-up (not shown), the network structure and morph composition of the food web is practically static. It consists of several distinct bodysize clusters, each centred at a bodysize which is a multiple of the optimal feeding distance d. These clusters are analogous to trophic levels. In particular, a morph in a given cluster predominantly consumes morphs in the cluster immediately below it and, similarly, is mainly consumed by morphs in the cluster immediately above it. Trophic levels are further separated into sharp bodysize layers. That is, morphs in the same trophic level are separated by a bodysize distance of β, which allows them to avoid interference

competition (note that here β is much smaller than the optimal feeding distance d). In the left panel of Fig. 2a, we plot the average biomass of morphs of a given bodysize throughout the simulation. This distribution is composed of single peaks indicating that the morph composition is static after the initial build up of the network. The envelope of all peaks within a trophic level is bell shaped. This arises due to differences in growth rate within the trophic level; morphs close to the centre of a trophic level are at the optimal feeding distance to the centre of the trophic level below and thus are able to grow faster. The total biomass of a trophic level decreases with increasing bodysize, due to efficiency losses.

In the example given, the trophic levels are distinct. Increasing the feeding range σ, or competition strength α_0 causes the trophic levels to widen until the trophic levels merge. As the competition range β increases, the bodysize distance between morphs within a trophic level increases and fewer morphs can coexist in each level. For sufficiently large β only a single morph can exist in the system and we enter region II.

Single morph cycles: region II. For large competition ranges β (region II) we observe a new dynamic regime for this model, which we term single morph cycles. This regime is characterized by a dynamic monomorphic community that consists of the basal resource (of bodysize $z_0 = 0$) and a single consumer morph with a bodysize that is not constant but undergoes an evolutionary cycle, see Fig. 2b. The inset shows a close-up of the time series which displays the bodysize cycle more clearly. In addition, a close-up of the temporal evolution of the bodysize and biomass over four complete periods of the cycle is shown in the Appendix (Fig. A.5). At the beginning of a cycle, starting with a small initial bodysize, the resident is repeatedly replaced by a slightly larger morph. As the resident's bodysize increases, its biomass decreases, as seen in the trapezoidal structure of the biomass-bodysize distribution in the left panel of Fig. 2b and in Fig. A.5b in the Appendix. At the end of a cycle, the now large resident is invaded and outcompeted by a small mutant and the single morph cycle resets. The mechanism underlying this behaviour is discussed in Section 3.2. In contrast to region I, the biomass-bodysize distribution is continuous and not composed of single peaks, because morphs occur across the whole bodysize range of a cycle.

With increasing competition strength α_0 the frequency and amplitude of the cycle decrease (not shown). The amplitude also decreases with decreasing feeding range σ, but cycles are still present for $\sigma < 0.5$. We note that the

competition range β always encompasses the entirety of the bodysize range of a single morph cycle. As β decreases we eventually reach a threshold where the system can support a polymorphic food web and enter either region I or region III.

Complex community dynamics and coevolutionary cycles: regions III and IV. For low competition strength α_0 and small to intermediate competition range β we obtain a regime of complex community dynamics (region III), characterized by polymorphic food webs which are evolutionarily dynamic. Example time series for this region are plotted in Figs. 2c and d. In this regime, each trophic level within the food web undergoes an evolutionary cycle. This can be a single morph cycle, as described in the previous section (e.g., the lowest trophic level in Fig. 2d), or a coevolutionary cycle, in which the trophic level consists of multiple coevolving morphs (e.g., the lowest trophic level in Fig. 2c).

A close-up of the temporal dynamics of bodysizes and biomasses during a coevolutionary cycle is shown in Fig. 3. At the beginning of the cycle, the bodysizes of all morphs within the trophic level increase gradually in successive interdependent mutational steps, while maintaining a constant bodysize distance equal to the competition range. Initially this increase is gradual until, eventually, the largest morph goes extinct. The remaining morphs then rapidly increase their bodysize to fill this vacated niche. This effect cascades down to each of the smaller morphs allowing them to increase their bodysizes at a similar rate. This upwards movement also leaves a niche at small bodysize which a new morph can invade, which functionally resets the cycle to its initial state. The biomasses of the larger two morphs decrease as their bodysize increases (e.g. red curve in Fig. 3). This is because as their bodysize increases they move away from the optimal distance at which to feed on the next lowest trophic level. In contrast, the biomass of the smallest morph increases (e.g. blue or yellow curves), as it approaches the optimal feeding distance. The biomass of the intermediate morph (e.g. black or blue curves) stays relatively constant, as its bodysize moves from one side of the optimal feeding distance to the other.

While this describes the coevolutionary cycle within a trophic layer, different trophic levels within a food web undergo independent cycles. Fig. 2c, for example, shows a food web in which only coevolutionary cycles occur. The network has basically the same structure as in the static case, consisting of three trophic levels (Fig. 2a), but it is evolutionarily dynamic. Within a

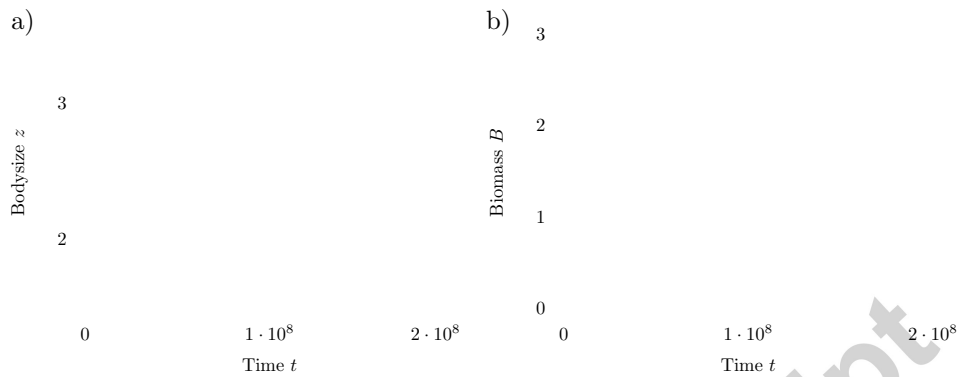

Figure 3: Evolutionary dynamics during a coevolution cycle. **a**) Close-up of the time evolution of morph bodysizes $z_i(t)$ within one trophic layer, here shown for the first trophic level of Fig. 2c. **b**) Corresponding time evolution of morph biomasses $B_i(t)$. Identical colours denote evolutionary akin morphs. The vertical lines mark time instances at which the two largest morphs in this trophic layer have a bodysize distance smaller than β. At these points the largest morph goes extinct and a new morph with smaller bodysize can invade the system.

trophic level, morphs coevolve, increasing their bodysize together, but these coevolutionary dynamics seem to be independent of the cycling within other trophic levels. In particular, the frequency of these cycles decreases with trophic level; about two or three cycles of the lowest trophic level occur for every single cycle of intermediate trophic level, while the highest trophic level is nearly static. This decrease reflects the fact that the overall mutation rate decreases with trophic level since, as observed in the static case (region I), the biomass of each successive trophic level is less than that of the previous one. In contrast to the static case, the cycling causes the biomass-bodysize distribution to become continuous as for single morph cycles (region II). This biomass distribution does not vary through a cycle, and, as a consequence the cycling of lower trophic levels does not influence higher trophic levels.

Coevolution cycles arise in food webs when the competition strength α_0 and the competition range β are low (see Fig.1). They also occur if α_0 is zero. As for single morph cycles, when α_0 increases the frequency and amplitude of a coevolution cycle decreases, until at sufficient large values of α_0 the different trophic layers of the food web become evolutionarily static in a series of successive infinite period bifurcations. Finally, when a critical threshold is passed the system enters region I. On the other hand, starting again in region III, with increasing β fewer morphs can exist in a trophic level (in an analogous way to that described in Section 3.1). As a consequence, the

frequency of these cycles slightly increases with β because with decreasing number of morphs but constant nutrient input, each morph can acquire a higher biomass, which increases the mutation rates and the evolutionary speed. Finally, for sufficiently large β we observe the collapse of the whole polymorphic system into a single morph cycle (region II).

For intermediate values of β, it is also possible for the lowest trophic level to transition to single morph cycles, while the other trophic levels are unaffected, see Fig. 2d. We call such cases mixed evolutionary cycles. Food webs undergoing mixed evolutionary cycling have clear similarities to those displaying purely coevolutionary cycling. In Fig. 2d we still see three distinct trophic levels with continuous biomass-bodysize distributions. However, the upper two trophic levels are much closer together than in the purely coevolutionary case. In addition, while the biomass-bodysize distributions of these levels remain bell shaped the distribution for the lower trophic level is approximately rectangular, a clear precursor to the trapezoidal form obtained for single morph cycles, see Fig. 2b. Note that the lower trophic level can occasionally support a second resident, see Fig. 2d at time $t = 5 \cdot 10^8$. The single morph cycle stops and both residents increase in bodysize. Eventually the bigger morph goes extinct, as in a coevolution cycle, and the single morph cycle starts again. The origin of mixed evolutionary cycles can be explained by the observation that the lowest trophic level is subject to especially strong predation pressure because its residents can be consumed by morphs in all higher trophic levels. Predation and competition strength, α_0, have the same structure, so the effect of higher predation is similar to imposing a higher value of α_0 on the lowest trophic level. As a consequence, by comparison with Fig. 1, this trophic level can collapse into a single morph cycle for a value of β at which the higher trophic levels still perform coevolutionary cycles.

The transition into region II, by further increase of β, is characterized by a region of transient single morph cycles (region IV). In this regime, we can observe single morph cycles that persist only for a finite time and eventually become polymorphic. The resulting polymorphism can be either evolutionarily static or dynamic, depending on the competition strength α_0. If decreasing β returns the system to region III, as above, we obtain a mixed evolutionary cycle (see example time series in Fig. A.6a). Alternatively, if decreasing β returns the system to region I then we will obtain a static food web (see Fig. A.6b). As β increases, the probability that a polymorphic state emerges from these single morph cycles declines, eventually reaching zero as

the system enters region II.

3.2. Invasion analysis

Anatomy of a Single Morph Cycle. The existence of evolutionarily dynamic food webs has not previously been observed in this model. In this section we seek to develop an understanding of these dynamic states. We start by considering single morph cycles, which are characterized by a monomorphic system that undergoes a sequence of replacements of a resident, z_R, by a slightly larger mutant, z_M. Eventually this gradual increase in resident bodysize ends when a small morph is able to invade and the cycle resets (Fig. 2b). To gain insight into this process, we consider the invasion fitness $s(z_M, z_R)$ of a mutant z_M in a monomorphic system of bodysize z_R [14]. The invasion fitness $s(z_M, z_R)$ can be derived from Eq. (1) and is given by:

$$\begin{aligned} s(z_M, z_R) =& f(z_M)\ \gamma(z_M)B_0 + f(z_M)\ \gamma(z_M - z_R)B_R - m(z_M) \\ & - \gamma(z_R - z_M)B_R - \alpha(|z_M - z_R|)B_R. \end{aligned} \tag{5}$$

Here, B_0 and B_R denote the equilibrium biomasses of the resource and the resident in the monomorphic system and are given by Eqs. (1) and (4). To gain analytically tractable expressions for the invasion fitness, we neglect the nutrient recycling terms in Eq. (4), that is we take ν equal to zero.

A positive invasion fitness $s(z_M, z_R) > 0$ indicates that the mutant is able to invade and establish itself. Assuming that the population stays monomorphic, we can use Eq. (5) to construct the bodysize ranges which characterize a viable mutant for a given resident bodysize. These ranges can be summarized graphically using Pairwise Invasibility Plots (PIP) [14]. In Fig. 4a we plot a PIP for the parameter set used to obtain Fig. 2b. Using this PIP we find that the evolutionary cycle can be split into two phases as follows. Phase 1: For small resident bodysizes ($z_R < 3.54$) only mutants with larger bodysizes have positive fitness. Thus, the resident's bodysize increases over evolutionary time via a series of replacements by a larger mutant (blue arrow in Fig. 4a). Phase 2: When the resident's bodysize reaches a critical value ($z_R \geq z_J = 3.54$), a second positive fitness region emerges corresponding to mutants which are smaller than the resident. At this point a jump to a smaller bodysize becomes possible (green arrows in Fig. 4a). Such a jump can produce a resident morph small enough to return the cycle to its initial

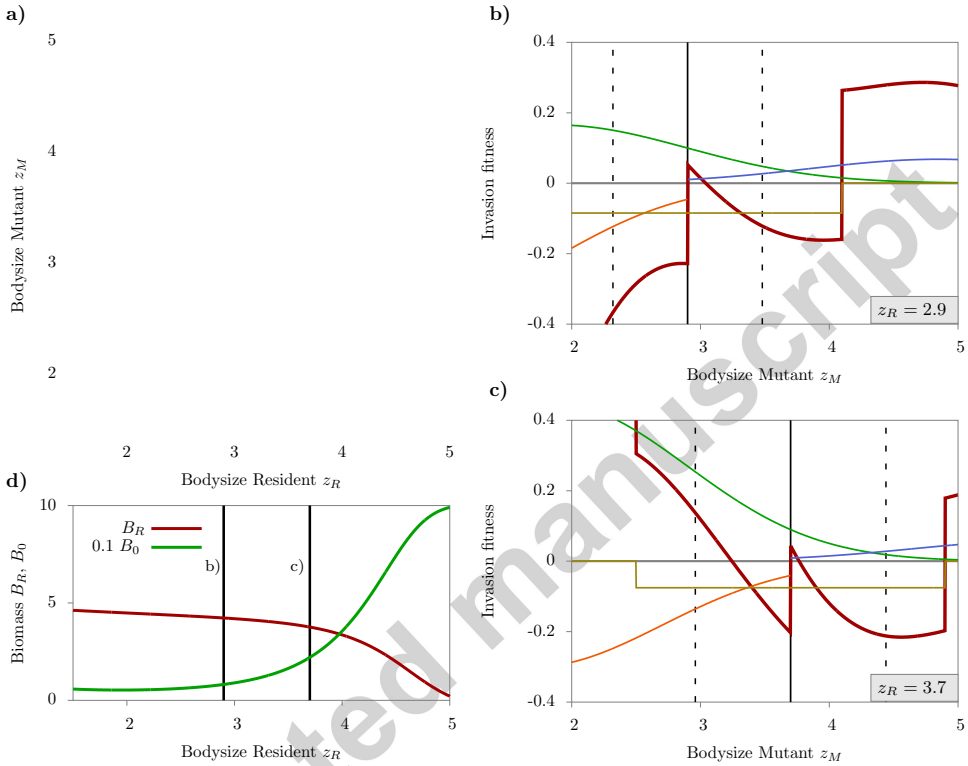

Figure 4: Invasion analysis of a single morph cycle. **a**) Pairwise Invasibility Plot (PIP) in dependence of the bodysize of the resident z_R and of the mutant z_M. Regions with negative invasion fitness, $s(z_M, zR) < 0$, are marked in white and regions with $s(z_M, zR) > 0$ in grey. The bold line designates the points at which mutant and resident have identical bodysizes ($z_M = z_R$), dashed lines enclose the mutation interval ($0.8z_R$ and $1{,}2z_R$), and dashed-dotted lines the competition range ($z_R \pm \beta$). The arrows outline trajectories during a single morph cycle. The shaded areas delineate the variance of bodysizes during a cycle, where a resident may exceed the jump point (blue shaded area) or have varying initial bodysize (green shaded area). **b**, **c**) Fitness landscape as a function of the mutant's bodysize z_M, at the beginning of a cycle for $z_R = 2.9$ (**b**) and close to the end for $z_R = 3.7$ (**c**). The plot shows the invasion fitness (red) and its composition by growth due to resource consumption (green) and predation (blue) and by losses due to predation (orange), and interference competition (yellow), according to Eq. (5). For visualization all growth terms are rescaled by a factor of 0.2. The vertical solid line marks the bodysize z_R of the resident and the two dashed lines border the mutation interval. **d**) Equilibrium biomass of the resident, B_R, and of the resource, B_0, as a function of z_R. The vertical lines mark the values of z_R corresponding to panels b) and c). Parameter values are $\beta = 1.2$, $\alpha = 0.1$, corresponding to Point 2b in Fig. 1.

state. Having outlined the cycle we now consider its two phases in more detail.

In Fig. 4b we plot the invasion fitness (i.e., a cross-section of the PIP) for a typical point ($z_R = 2.9$) in Phase 1 of the cycle. The dependence of the invasion fitness $s(z_M, z_R)$ on the bodysize of the mutant z_M (red curve) shows a non-monotonic behaviour, which can be explained by the way in which $s(z_M, z_R)$ is composed by different gain and loss terms in Eq. (5). We see that the effects of intrinsic mortality (purple) and competition (grey) are relatively constant with respect to mutant bodysize, at least within the mutation interval. Note though, that the competition loss disappears for $z_M > z_R + \beta$, giving rise to the upward jump of the invasion fitness at $z_M = 4.1$. Here, this region of increased invasion fitness is outside of the mutation interval and does not interfere with the single morph cycle. Growth due to resource consumption (green) declines gradually with mutant size, as larger morphs have lower resource feeding efficiency (the size difference becomes larger than the optimal feeding distance $z_M - z_0 > d$). The most significant factor is the effect of asymmetry in the predation interactions. In particular, mutants that are larger than the resident are able to increase their growth by feeding on it (blue), while mutants smaller than the resident suffer from predation by the resident (orange). This results in an upward jump of the invasion fitness at $z_M = z_R$, which is sufficient to off-set the moderated decay in feeding efficiency creating a region of positive invasion fitness for increased bodysizes $z_M > z_R$. Consequently, the only viable evolutionary path in Phase 1 is increasing bodysize (blue arrow).

With increasing bodysize of the resident z_R, the decline in the feeding efficiency on the resource becomes more severe because the deviation from the optimal feeding distance to the resource increases. As a consequence, the invasion fitness is increasingly dominated by the relative contribution of the feeding efficiency (green). In contrast, the jump in the invasion fitness at $z_M = z_R$ due to the asymmetry of predation remains largely independent of z_R. As a consequence, the region of positive fitness for larger mutants ($z_M > z_R$) shrinks with increasing z_R (see Figs. 4a and c). Using analytical and numerical calculations (not shown) we found that this region finally disappears for a resident bodysize of $z_{max} = 5.09$ (independent of the competition parameters α_0 and β). As such z_{max} is the maximal achievable bodysize of a morph in a monomorphic system for the given parameter values. Furthermore note that the probability of an evolutionary change, and hence the speed of the evolutionary dynamics, is proportional to the ratio

of the positive fitness interval to the mutation interval. Thus, as the fitness interval for larger morphs shrinks, the rate of increase in resident bodysize decreases, going to zero as z_R approaches z_{max}.

These effects stem from the apparently paradoxical observation that, while increasing bodysize is evolutionarily favoured, it results in a less fit resident. The larger resident's lower feeding efficiency results in it being less able to exploit the remaining resource at z_0. Consequently, as resident bodysize, z_R, increases, resident biomass and utilization of the resource decline. This effect can be seen clearly by plotting resident and resource biomass against resident bodysize, see Fig. 4d.

The increased availability of the resource is responsible for the emergence of a second positive fitness interval found in Phase 2 of the cycle. A typical invasion fitness profile is plotted in Fig. 4c. The contributions of most growth factors are similar to those obtained in Phase 1 (Fig. 4b). However, now the growth due to resource consumption depends more strongly on mutant size and its maximum contribution is much higher. For sufficiently small mutants the extra growth gained from greater feeding efficiency is able to off-set the increased losses from predation, allowing a smaller mutant to displace the resident (green arrows). We refer to the smallest resident bodysize for which this is possible as the jump point z_J (for the chosen parameter values $z_J = 3.54$). When a mutant with bodysize less than this threshold successfully invades the system, the system resets to Phase 1.

Note that, since mutational steps are random, the range of bodysizes during an evolutionary cycle varies. The resident's bodysize can exceed the jump point before the smaller mutant invades (blue shaded area in Fig. 4a). Furthermore, the smaller mutant can occur anywhere within the positive region of the fitness cross-section obtained for a given resident. The combination of these two effects allows the smaller mutant to emerge in a relatively wide range (green shaded area in Fig. 4a).

We observed previously that the frequency of single morph cycles was related to the competition strength α_0. This can now be explained as follows. Note first that once the jump point is reached the cycle can be reset in a single step. Furthermore, such a reset has a high probability, since the positive fitness region for the smaller mutant is bigger than that for a larger mutant. Thus, the system is unlikely to spend a significant amount of evolutionary time in Phase 2. Consequently, the length of a cycle is primarily determined by the number of evolutionary steps required to produce a resident with bodysize greater than z_J. The region of positive fitness larger than

the resident, which is responsible for the upwards movement (see Figs. 4a and c), narrows with increasing competition strength α_0 (because the fitness landscape is shifted downwards within the competition range). Therefore increasing the competition strength reduces the evolutionary speed and thus the frequency of the cycle.

In summary, the intrinsic asymmetry in the feeding kernel $\gamma(\cdot)$ in Eq. (3) creates an evolutionary ratchet, which results in an increase in the resident's bodysize. However, the concomitant decrease in resident feeding efficiency generates a nutrient environment which ultimately allows the invasion of a small mutant. The interplay between these two processes results in a single morph evolutionary cycle.

Transition region to dimorphic states. While in single morph cycles the mutant always replaces the resident, we observed that in region IV single morph cycles can become polymorphic. While the dynamics of such a polymorphic state are analytically intractable (at least using the techniques outlined above), we are able to determine conditions under which a dimorphic state can form. In particular, in this model two species are able to coexist only if they do not compete directly; that is if the distance between their bodysizes is greater than the competitive range, β. Thus a dimorphism becomes possible when the mutation interval, $[0.8z_R, 1.2z_R]$, contains the competition interval, $[z_R - \beta, z_R + \beta]$. We call the smallest resident bodysize where this condition holds the dimorphic point, z_D, and note that it is related to the competition range as follows, $z_D = 5\beta$. With this in mind the transitory single morph cycles found in region IV can be explained by the random nature of the mutational steps. In particular, when $z_D > z_J$ the resident bodysize must increase past z_J in order to reach the dimorphic point. Consequently the system must enter Phase 2 and thus the possibility of the cycle resetting before the system becomes polymorphic exists. The further above z_D is from z_J the more likely it becomes that the cycle resets before it becomes dimorphic. This intuition is justified formally below.

In Fig. 1, we plotted the probability of a single morph cycle becoming dimorphic during a single cycle. This probability was estimated as follows: for a fixed resident bodysize, the probability for a given mutational step attaining a particular evolutionary outcome (dimorphism, upwards or downwards movement in bodysize) is given by the range in the invasion fitness that leads to the evolutionary event divided by the whole positive fitness area. The negative fitness area is not considered since an unsuccessful invasion does not

alter the system. We start with a resident of a bodysize of z_J and calculate the probability of each evolutionary outcome (transition probability) for that resident bodysize. In the next step, we increase the resident bodysize by the expected mutational step-size of the upwards movement. (This is given by the centre of the positive fitness responsible for upwards movement.) Thus we calculate the transition probabilities at each of the expected bodysizes between z_J and z_{max} and by doing this consecutively we consider all possible evolutionary trajectories. These trajectories terminate when a dimorphism emerges or the cycle resets (which is assumed to happen via a downwards movement). The probability to become dimorphic along a given trajectory is equal to the product of the transition probabilities of the steps in that trajectory. The overall probability of reaching a dimorphic state is then given by summing over all trajectories which reach this state.

Complex Community Dynamics. In region III we observe food webs that contain coevolutionary, and occasionally single morph, cycles. We have previously observed that the cycles in distinct trophic levels are independent. As such the behaviour of single morph cycles, even in a polymorphic system, can be adequately understood in a monomorphic context, see above. Moreover, the dynamic patterns of coevolutionary cycles can be understood in terms of the evolutionary behaviour of morphs in a single trophic level. The increase of a morph's bodysize in a coevolution cycle is due to the same mechanism as in single morph cycles. The asymmetry in the feeding kernel $\gamma(\cdot)$ (Eq. (3)), creates an evolutionary ratchet, which drives the morphs to higher bodysizes (see Fig. 3). However, the evolution of the morphs is limited by interference competition. Each morph, except the largest and the smallest morph, have two neighbours at a bodysize distance slightly bigger than the competition range β. Therefore mutants of the intermediate morphs inevitably compete with these neighbours and can not invade. While the smallest morph has only a larger neighbour, smaller mutants are not viable due to the decreasing ability to feed on the lower trophic level and high intra trophic level predation. The largest morph in an coevolution cycle has only a smaller neighbour, thus it can increase its bodysize through the evolutionary ratchet. All other morphs follow one after another, since they are not bounded upwards any more. Therefore coevolution is a top-down process in this model. However, just as in the single morph case, increasing bodysize results in the largest morph reaching an unstable state where it can be invaded and outcompeted by smaller mutants. This is analogous to the jump point of a single morph

cycle.

In contrast to single morph cycles, the largest resident is not outcompeted by a new offspring of its own, but by a mutant of the second largest resident. The second largest resident is replaced by a slightly larger mutant, which is within competition range β of the largest resident. (Time-points, at which the two largest residents compete are marked by grey vertical lines in Figs. 2c and 3.) This mutant is close enough to the optimal feeding distance that it can outcompete, and thus replace, the largest resident. Thus the interference competition from above is removed, allowing each of the resident morphs to increase its bodysize. A new mutant, descended either from the smallest resident, or from a resident in a lower trophic level, can invade either close to the end, or at the beginning, of a cycle; when the interference competition from the smallest resident is lowest.

4. Discussion

The model introduced by Loeuille and Loreau [20] is well known for evolutionarily static food webs. We investigated a larger range of competition parameters, and found novel evolutionary states: cycling of single morphs (region II), cycling of complete food webs (region III), and transitory states from single morph cycles to polymorphic food webs (region IV). We want to discuss six main implications of our study:

First, the observed evolutionary cycles are based on coevolution, which is driven by competition and trophic interactions between resident morphs and also the invader. These coevolutionary processes are observed in empirical studies, where they can also be driven by competition [9, 23] or trophic interactions [1]. However, it is hard to study coevolution empirically in larger communities, due to the high number of complex interactions which make identification of the evolutionary dynamics and the coevolving traits very difficult [33]. Our findings show that it is not necessary to consider all interactions between species within the community to explain cycling. Instead, it is sufficient to consider interactions between smaller, independently coevolving, subgroups. In our system, each trophic level represents a subgroup, since each level evolves independently with a different frequency.

Second, we found that food web characteristics are remarkably robust towards evolution. The network structure, number of morphs and links are relatively constant during evolution. In addition, the network structures of solely coevolving food webs and static food webs are similar. Therefore

they are not distinguishable on the time scale of the population dynamics. However for mixed evolutionary food webs the network structure changes: the number of species contained in each trophic level and the distance between each level loses its regularity.

Third, our results are in agreement with Cope's rule [10]: During an evolutionary cycle, morphs increase their bodysize, since a slightly larger morph has a higher fitness than a smaller morph. In addition, our study suggests a more natural explanation of the "Endless trends to gigantism" paradigm [16] than mass extinction [18]. Large bodysizes are advantageous over a wide range, especially towards similar sized morphs, but result in a lower ability to consume the original resource, which finally increases the vulnerability towards invasion of better adapted morphs.

Fourth, single morph cycles have similar characteristics to taxon cycles [34, 45], suggesting that the down-regulation of the environmental quality for the resident (decreasing resource consumption) is also responsible for the arising evolutionary cycling: the increase in bodysize of the resident, due to coevolution with invaders, results in morphs that are progressively less suited to their environment. Thus, morphs that are better adapted to the environment can invade. Furthermore, theoretical studies of competing species on a niche axis have shown that this class of evolutionary community cycles is related to the asymmetry in the competitive interaction (Rummel and Roughgarden [35], Taper and Case [41], Matsuda and Abrams [24]). In our study an asymmetry is introduced naturally via trophic interactions and therefore we suggest that evolutionary cycling is an intrinsic phenomenon in the model of Loeuille and Loreau [20], which can also occur in the absence of competition. Evolutionary cycling might be a general phenomenon in evolutionary size-structured food web models.

Fifth, our study provides a new avenue for the debate of whether ongoing evolutionary changes and Red Queen dynamics are ecologically realistic. Dieckmann et al. [12] proposed evolutionary limit cycles, e.g between predator and prey species, as a theoretical framework for Red Queen dynamics, but our study suggests an alternative mechanism. Thereby, in the simplest case of single morph cycles, the resident species is evolutionarily driven towards unfavourable positions in niche space, which reduces its viability and ultimately leads to self-extinction - so that the community can be colonized again by a mutant or invader at a different, more favorable, phenotypic trait. In contrast, in even the simplest predator-prey limit cycle, both species are present at all times.

Sixth, we propose that taxon cycles might be a transitory phase of island colonisation: we observe that single morph cycles can be transitory states, after which the community becomes polymorphic and large food webs emerge. These webs can be either static or dynamic. The latter can be a possible representation of cycling of larger communities – continental taxon cycles – which are hypothesised, but hard to study empirically, due the intertwining of the invasion processes [29]. Note that within the model used, the estimation of the time scale considered is not possible without relating it to empirical data, since all variables are treated as dimensionless.

As with all modelling studies, our results depend on the choice of process formulations and simplifications used in the model. Here, we have chosen to closely follow the formulation as defined by Loeuille and Loreau [20]. While many compelling refinements of this model have been proposed [21, 20, 4, 8, 5], our study shows that evolutionary community cycles are already a natural outcome in the original model. Using extensive numerical simulations we have confirmed that our main model results also hold in more refined model variants. We briefly mention the two most influential changes: to the competition and feeding kernels. First, following Loeuille and Loreau [20] we have used a box-shaped kernel $\alpha(\cdot)$ with a finite competition range β to describe the interference competition (Eq. (3)). Therefore, morphs either compete with a fixed, well-defined strength, or competition is absent. More realistically, competition strength should change continuously with bodysize distance which could be described by link overlap (e.g. a Gaussian kernel) sensu [22], as applied by [5, 8, 30]. Using numerical simulations we verified that evolutionary cycling still occurs if the box-shaped interference competition is replaced by link overlap competition. Furthermore, the range of link overlap competition is closely related to the feeding range σ of the competing morphs ($\propto \sqrt{2}\sigma$). Comparing link overlap competition with box-shaped competition shows that link overlap competition occurs over a wider bodysize distance. This justifies the investigated competition range β in our studies.

Second, following Loeuille and Loreau [20], our chosen feeding kernel $\gamma(\cdot)$ consists of a truncated Gaussian. This discontinuity could be responsible for the cycling behaviour observed. However, when the discontinuous feeding and competition kernels were replaced with continuous functions, we still observed cycling see Fig. A.7. In particular, we note that it was necessary to use an asymmetric feeding kernel (the ability to consume morphs with a larger bodysize decreases faster than the ability to consume smaller morphs) e.g. the Ricker function [44], in order to obtain this behaviour. Thus, we

conclude that cycling behaviour arises from strong asymmetries in the feeding kernel.

We have shown that evolutionary cycles occur in the evolutionary food web model used, it is robust towards variation in the shape and range of the feeding and competition kernels, and can manifest in various ways. However, the underlying mechanism, leading to evolutionary cycling, is not restricted to the model used. We suggest that evolutionary cycles might be a general phenomenon in evolutionary food web models and also empirical food webs and therefore conclude that evolutionary cycling in food webs may be more frequent than commonly believed.

Acknowledgements

This work was supported by: the DFG, as part of the research unit 1748; and by the Ministry of Science and Culture of Lower Saxony, in the project Biodiversity-Ecosystem Functioning across marine and terrestrial ecosystems.

[1] Abrams, P.A., 2000. The evolution of predator-prey interactions: Theory and evidence. Annual Review of Ecology and Systematics 31, 79–105. doi:10.1146/annurev.ecolsys.31.1.79.

[2] Abrams, P.A., Matsuda, H., 1997. Prey adaptation as a cause of predator-prey cycles. Evolution 51, 1742–1750.

[3] Abrams, P.A., Matsuda, H., Harada, Y., 1993. Evolutionarily unstable fitness maxima and stable fitness minima of continuous traits. Evolutionary Ecology 7, 465–487. doi:10.1007/BF01237642.

[4] Allhoff, K.T., Drossel, B., 2013. When do evolutionary food web models generate complex networks? Journal of Theoretical Biology 334, 122 – 129. doi:10.1016/j.jtbi.2013.06.008.

[5] Allhoff, K.T., Ritterskamp, D., Rall, B. C. Drossel, B.G.C., 2015. Evolutionary food web model based on body masses gives realistic networks with permanent species turnover. Scientific Report 5. doi:10.1038/srep10955.

[6] Bonsall, M.B., Jansen, V.A.A., Hassell, M.P., 2004. Life history trade-offs assemble ecological guilds. Science 306, 111–114. doi:10.1126/science.1100680.

[7] Brännström, A., Johansson, J., 2012. Modelling the ecology and evolution of communities: a review of past achievements, current efforts, and future promises. Evolutionary Ecology Research 14, 601–625.

[8] Brännström, A., Loeuille, N., Loreau, M., Dieckmann, U., 2011. Emergence and maintenance of biodiversity in an evolutionary food-web model. Theoretical Ecology 4, 467–478. doi:10.1007/s12080-010-0089-6.

[9] Connell, J.H., 1980. Diversity and the coevolution of competitors, or the ghost of competition past. Oikos 35, 131–138. doi:10.2307/3544421.

[10] Cope, E.D., 1896. The primary factors of organic evolution. volume 2. University of Michigan Library.

[11] Dieckmann, U., Doebeli, M., 1999. On the origin of species by sympatric speciation. Nature 400, 354–7. doi:10.1038/22521.

[12] Dieckmann, U., Marrow, P., Law, R., 1995. Evolutionary cycling in predator-prey interactions: population dynamics and the red queen. Journal of theoretical biology 176, 91–102. doi:10.1006/jtbi.1995.0179.

[13] Fussmann, G.F., Loreau, M., Abrams, P.A., 2007. Eco-evolutionary dynamics of communities and ecosystems. Functional Ecology 21, 465–477. doi:10.1111/j.1365-2435.2007.01275.x.

[14] Geritz, S., Kisdi, E., Mesze, G., Metz, J., 1998. Evolutionarily singular strategies and the adaptive growth and branching of the evolutionary tree. Evolutionary Ecology 12, 35–57. doi:10.1023/A:1006554906681.

[15] Gyllenberg, M., Parvinen, K., Dieckmann, U., 2002. Evolutionary suicide and evolution of dispersal in structured metapopulations. Journal of Mathematical Biology 45, 79–105. doi:10.1007/s002850200151.

[16] Hone, D.W., Benton, M.J., 2005. The evolution of large size: how does cope's rule work? Trends in Ecology & Evolution 20, 4 – 6. doi:10.1016/j.tree.2004.10.012.

[17] Jansen, V.A.A., Mulder, G., 1999. Evolving biodiversity. Ecology Letters 2, 379–386. doi:10.1046/j.1461-0248.1999.00100.x.

[18] Kingsolver, J.G., Pfennig, D.W., 2004. Individual-level selection as a cause of cope's rule of phyletic size increase. Evolution 58, 1608–1612. doi:10.1111/j.0014-3820.2004.tb01740.x.

[19] Kisdi, E., Jacobs, F., Geritz, S., 2002. Red Queen evolution by cycles of evolutionary branching and extinction. Selection 2, 161–176. doi:10.1556/Select.2.2001.1-2.12.

[20] Loeuille, N., Loreau, M., 2005. Evolutionary emergence of size-structured food webs. Proceedings of the National Academy of Sciences of the United States of America 102, 5761–5766. doi:10.1073/pnas.0408424102.

[21] Loeuille, N., Loreau, M., 2006. Evolution of body size in food webs: does the energetic equivalence rule hold? Ecology Letters 9, 171–178. doi:10.1111/j.1461-0248.2005.00861.x.

[22] MacArthur, R., Levins, R., 1967. The limiting similarity, convergence, and divergence of coexisting species. The American Naturalist 101, 377–385.

[23] MacArthur, R.H., 1957. On the relative abundance of brid species. Proceedings of the National Academy of Sciences of the United States of America 43, 293–295.

[24] Matsuda, H., Abrams, P.A., 1994. Runaway evolution to self-extinction under asymmetrical competition. Evolution 48, 1764–1772. doi:10.2307/2410506.

[25] Parvinen, K., 2005. Evolutionary suicide. Acta Biotheoretica 53, 241–264. doi:10.1007/s10441-005-2531-5.

[26] Peters, R.H., 1986. The Ecological Implications of Body Size (Cambridge Studies in Ecology). Cambridge University Press.

[27] Pimentel, D., 1961. Animal population regulation by the genetic feedback mechanism. The American Naturalist 95, 65–79.

[28] Press, W.H., Teukolsky, S.A., Vetterling, W.T., Flannery, B.P., 2007. Numerical Recipes 3rd Edition: The Art of Scientific Computing. Cambridge University Press.

[29] Ricklefs, R.E., Cox, G.W., 1972. Taxon cycles in the west indian avifauna. The American Naturalist 106, 195–219.

[30] Ritterskamp, D., Bearup, D., Blasius, B., 2016. A new dimension: Evolutionary food web dynamics in two dimensional trait space. Journal of Theoretical Biology , in press, doi:10.1016/j.jtbi.2016.03.042.

[31] Rosenzweig, M.L., 1978. Competitive speciation. Biological Journal of the Linnean Society 10, 275–289.

[32] Rossberg, A., H, M., Amemiya, T., Itoh, K., 2006. Food webs: Experts consuming families of experts. Journal of Theoretical Biology 241, 552 – 563. doi:10.1016/j.jtbi.2005.12.021.

[33] Rothstein, S.I., 1990. A model system for coevolution: Avian brood parasitism. Annual Review of Ecology and Systematics 21, 481–508. doi:10.1146/annurev.es.21.110190.002405.

[34] Roughgarden, J., Pacala, S., 1989. Taxon cycle among anolis lizard populations: review of evidence, in: Otte, D., Endler, J.A. (Eds.), Speciation and its consequences. Sinauer Associates Inc, pp. 403–432.

[35] Rummel, J.D., Roughgarden, J., 1983. Some differences between invasion-structured and coevolution-structured competitive communities: A preliminary theoretical analysis. Oikos 41, 477–486.

[36] Rummel, J.D., Roughgarden, J., 1985. A Theory of Faunal Buildup for Competition Communities. Evolution 39, 1009–1033.

[37] Scheffer, M., van Nes, E.H., 2006. Self-organized similarity, the evolutionary emergence of groups of similar species. Proceedings of the National Academy of Sciences of the United States of America 103, 6230–5. doi:10.1073/pnas.0508024103.

[38] Slatkin, M., 1980. Ecological character displacement. Ecology 61, 163–177.

[39] Takahashi, D., Brännström, A., Mazzucco, R., Yamauchi, A., Dieckmann, U., 2011. Cyclic transitions in simulated food-web evolution. Journal of Plant Interactions 6, 181–182. doi:10.1080/17429145.2011.552794.

[40] Takahashi, D., Brännström, A., Mazzucco, R., Yamauchi, A., Dieckmann, U., 2013. Abrupt community transitions and cyclic evolutionary dynamics in complex food webs. Journal of Theoretical Biology 337, 181 – 189. doi:10.1016/j.jtbi.2013.08.003.

[41] Taper, M., Case, T., 1992. Models of character displacement and the theoretical robustness of taxon cycles. Evolution 46, 317–333.

[42] Taper, M.L., Chase, T.J., 1985. Quantitative genetic models for the coevolution of character displacement. Ecology 66, 355–371.

[43] Van Valen, L., 1973. A new evolutionary law. Evolutionary Theory 1, 1–30.

[44] Vucic-Pestic, O., Rall, B.C., Kalinkat, G., Brose, U., 2010. Allometric functional response model: body masses constrain interaction strengths. Journal of Animal Ecology 79, 249–256. doi:10.1111/j.1365-2656.2009.01622.x.

[45] Wilson, E.O., 1961. The nature of the taxon cycle in the melanesian ant fauna. The American Naturalist 95, 169–193.

[46] Zhang, L., Andersen, K.H., Dieckmann, U., Brännström, A., 2015. Four types of interference competition and their impacts on the ecology and evolution of size-structured populations and communities. Journal of Theoretical Biology 380, 280–290. doi:10.1016/j.jtbi.2015.05.023.

Appendix A. Appendix

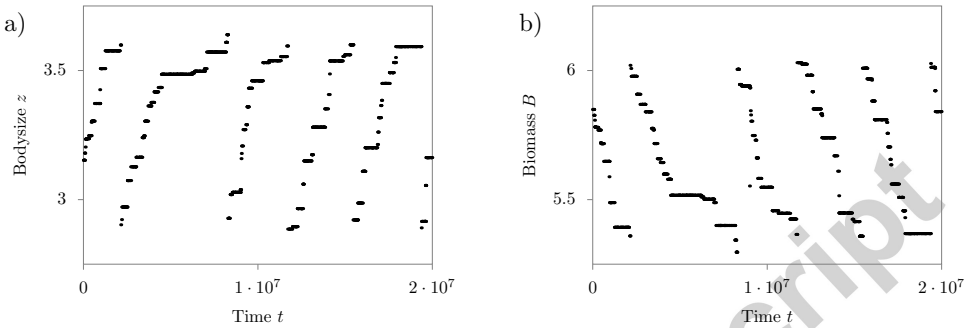

Figure A.5: Evolutionary temporal behaviour of a single morph cycle (Fig. 2b)). **a**, **b**: Close-up of the biomass B and bodysize z during a single morph cycle shown in Fig. 2b.

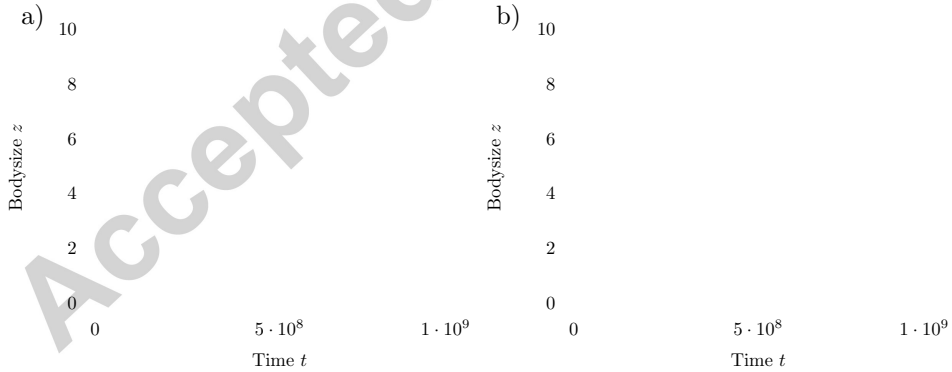

Figure A.6: Transient dynamic. After a transient of single morph cycles the system becomes polymorphic. **a**: Mixed evolutionary behaviour of a food web is visible after the transition. The competition parameters are set to $\alpha_0 = 0.1$ and $\beta = 0.75$. **b**: A static food web emerges after the transition. The competition parameters are set to $\alpha_0 = 0.3$ and $\beta = 0.58$.

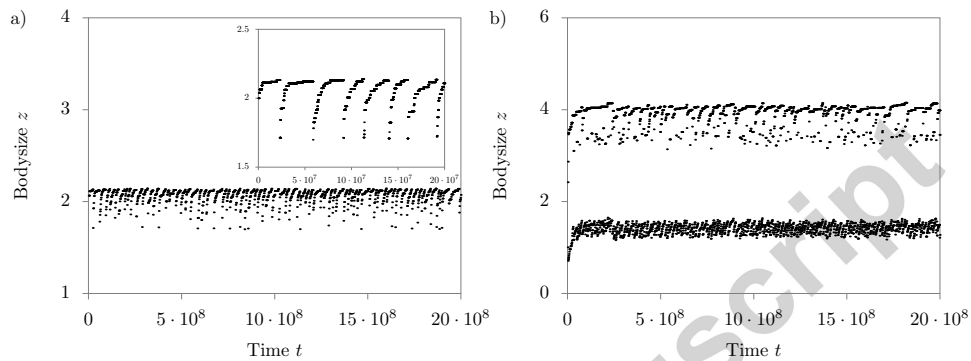

Figure A.7: Evolutionary food web behaviour for continuous feeding kernels. The interaction kernels are replaced by continuous functions. The original *feeding kernel* $\gamma(\cdot)$ (Eq. 2) is replaced by a more ecologically accurate Ricker function [44], $\gamma(z_i - z_j) = \frac{\gamma_0}{\sigma\sqrt{2\pi}} \exp\left(-\frac{(log(z_i - z_j) - log(d))^2}{\sigma^2}\right)$, which is asymmetric in respect to bodysize: the ability to consume larger morphs decreases faster than the ability to consume smaller morphs. The box shaped *competition kernel* $\alpha(\cdot)$ (Eq. 3) is replaced by a Gaussian function, $\alpha(|z_i - z_j|) = \frac{\alpha_0}{\beta\sqrt{2\pi}} \exp\left(-\frac{(z_i - z_j)^2}{\beta^2}\right)$, similar to [8, 5, 30]. The Gaussian shape is motivated by competition due to link overlap as introduced by [22]. It is highest for identical bodysizes and decreases with the bodysize distance of the competing morphs. **a:** Single morph cycle for continuous interaction kernels, which is similar to the one observed in the original model, Fig. 2b ($\sigma = 2.3, \alpha_0 = 0.2$, $\beta = 2$). **b:** Complex community cycles, that commemorate complex community cycles, see Fig. 2c,d ($\sigma = 2.5, \alpha_0 = 0.2$, $\beta = 1.5$). All other parameters are set according to section 2.3.